



HAL
open science

Nanocell type Ru@quinone core-shell catalyst for selective oxidation of alcohols to carbonyl compounds

J.P. P Zhao, W.Y. y Hernández, W.J. J Zhou, Y. Yang, E.I. I Vovk, M. Wu,
Negar Naghavi, M. Capron, V. Ordonsky

► To cite this version:

J.P. P Zhao, W.Y. y Hernández, W.J. J Zhou, Y. Yang, E.I. I Vovk, et al.. Nanocell type Ru@quinone core-shell catalyst for selective oxidation of alcohols to carbonyl compounds. *Applied Catalysis A : General*, 2020, 602, pp.117693. 10.1016/j.apcata.2020.117693 . hal-02926739

HAL Id: hal-02926739

<https://hal.science/hal-02926739>

Submitted on 23 Nov 2020

HAL is a multi-disciplinary open access archive for the deposit and dissemination of scientific research documents, whether they are published or not. The documents may come from teaching and research institutions in France or abroad, or from public or private research centers.

L'archive ouverte pluridisciplinaire **HAL**, est destinée au dépôt et à la diffusion de documents scientifiques de niveau recherche, publiés ou non, émanant des établissements d'enseignement et de recherche français ou étrangers, des laboratoires publics ou privés.

Journal Pre-proof

Nanocell type Ru@quinone core-shell catalyst for selective oxidation of alcohols to carbonyl compounds

J.P. Zhao, W.Y. Hernández, W.J. Zhou, Y. Yang, E.I. Vovk, M. Wu, N. Naghavi, M. Capron, V. Ordonsky



PII: S0926-860X(20)30286-6
DOI: <https://doi.org/10.1016/j.apcata.2020.117693>
Reference: APCATA 117693

To appear in: *Applied Catalysis A, General*

Received Date: 6 February 2020
Revised Date: 22 May 2020
Accepted Date: 3 June 2020

Please cite this article as: Zhao JP, Hernández WY, Zhou WJ, Yang Y, Vovk EI, Wu M, Naghavi N, Capron M, Ordonsky V, Nanocell type Ru@quinone core-shell catalyst for selective oxidation of alcohols to carbonyl compounds, *Applied Catalysis A, General* (2020), doi: <https://doi.org/10.1016/j.apcata.2020.117693>

This is a PDF file of an article that has undergone enhancements after acceptance, such as the addition of a cover page and metadata, and formatting for readability, but it is not yet the definitive version of record. This version will undergo additional copyediting, typesetting and review before it is published in its final form, but we are providing this version to give early visibility of the article. Please note that, during the production process, errors may be discovered which could affect the content, and all legal disclaimers that apply to the journal pertain.

© 2020 Published by Elsevier.

Nanocell type Ru@quinone core-shell catalyst for selective oxidation of alcohols to carbonyl compounds

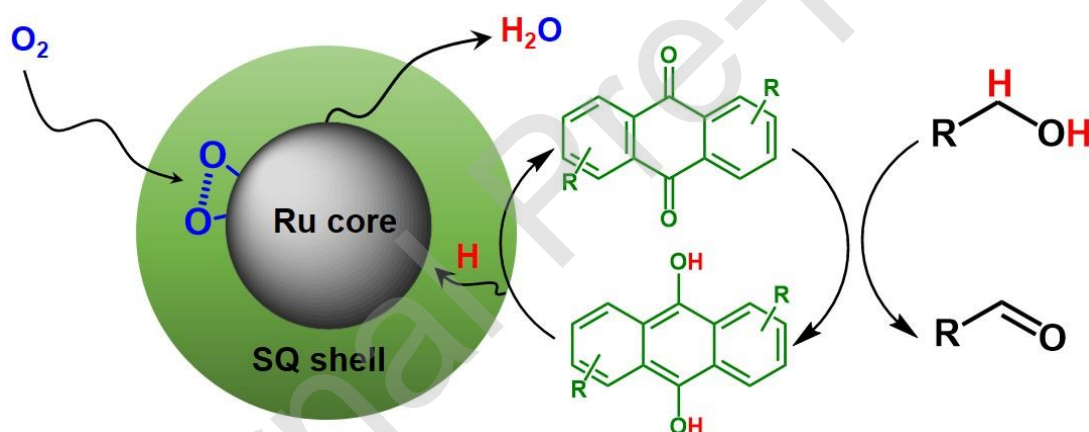
J.P. Zhao^{1,2}, W.Y. Hernández², W.J. Zhou², Y. Yang³, E.I. Vovk³, M. Wu², N. Naghavi², M. Capron^{1*}, V. Ordonsky^{2*}

¹Univ. Lille, CNRS, Centrale Lille, ENSCL, Univ. Artois, UMR 8181 - UCCS - Unité de Catalyse et Chimie du Solide, F-59000 Lille, France.

²Laboratoire, Eco-Efficient Products and Processes Laboratory (E2P2L), UMI 3464 CNRS-Solvay, 201108 Shanghai, China

³School of Physical Science and Technology, Shanghai Tech. University, 201210 Shanghai, China.

Graphical abstract



Highlights

- Ru nanoparticles coated by anthraquinone-2,6-disulfonate (SQ) have been prepared
- This catalyst selectively oxidizes different types of alcohols to aldehydes
- Strong interaction between Ru and SQ species changing electronic states was shown
- Mechanism involves abstraction by quinone of H with transfer to Ru core to form water

ABSTRACT:

Selective aerobic oxidation of alcohols to corresponding carbonyl compounds is one of the most important challenges in the modern chemical industry. The existing metal based heterogeneous catalysts provide low selectivity due to over-oxidation of aldehydes to acids and esters. We have found that coating of Ru nanoparticles by disodium anthraquinone-2,6-disulfonate (SQ) results in selective oxidation of aliphatic, unsaturated and aromatic alcohols to aldehydes. Analysis of core-shell Ru@SQ catalyst shows strong interaction between Ru and SQ leading to change of their electronic state and structure. *In-situ* study of alcohol oxidation using FTIR and electrochemistry indicates on hydrogen abstraction by shell quinone species with hydrogen transfer by quinone to Ru core for water generation. Thus, the catalyst behavior mimics nanoelectrocell by separation of oxidation reaction over quinone and reduction of oxygen over Ru providing higher selectivity to aldehyde.

Keywords: oxidation; alcohols; Ru; quinone; nanocell

Introduction

The selective oxidation of alcohols to versatile intermediates for the production of chemicals such as aldehydes and ketones remains a challenging task in the industry. It is of special interest the utilization of molecular oxygen as the green oxidant in the presence of a heterogeneous catalyst, thus favoring the atom economy in contrast to the use of toxic and expensive stoichiometric oxidants [1-5].

Different heterogeneous catalytic systems based on Pt [6-8], Pd [9, 10], Au [11, 12] have been reported for oxidation of alcohols. Among metallic catalysts, Ru has shown to be quite efficient in oxidation reactions [13-15]. However, low selectivity to aldehydes or ketones over heterogeneous catalysts is still a challenging problem due to formation of corresponding acids and esters [16]. The oxidation mechanism for metallic catalysts usually follows an oxidative dehydrogenation pathway, where both abstraction of hydrogen from alcohols and oxygen reduction processes (regeneration of the active site) simultaneously occur on the metal surface [17]. The aldehydes can be further oxidized over the same active sites to acids with decrease of the selectivity and

generation of waste products. In general, these catalysts are very efficient in the selective oxidation of activated alcohols (e.g. benzyl and allyl alcohols) but less active and selective for oxidation of aliphatic primary alcohols [18-21].

Recently, it has been found that metal-free electron deficient organic compounds like TEMPO (2,2,6,6-Tetramethylpiperidinyloxy) and DDQ (2,3-Dichloro-5,6-Dicyanobenzoquinone) can be used for dehydrogenation of alcohols in stoichiometric way, producing aldehydes and ketones together with the hydrogenated form of TEMPO and DDQ [22-25]. However, the use of large amounts of organic oxidants and difficulties related to their separation and regeneration strongly hinders the viability of this oxidation approach. To solve this drawback, the *in-situ* regeneration of these type of organic oxidants has been proposed, involving their combination with additional electron transfer mediators (ETM) and the utilization of a different terminal oxidant (e.g. oxygen). For example, Hu et al. explored an aerobic metal-free alcohol oxidation with a catalytic system consisting of TEMPO/Br₂/NaNO₂, where the Br₂/HBr redox pair oxidizes TEMPOH with subsequent regeneration by NO₂ [26]. In 1977, the DDQ-catalyzed reaction has been reported for the transformation of allylic alcohols to α,β -unsaturated ketones using 10 mol% DDQ in the presence of 30 mol% periodic acid under biphasic conditions at room temperature [27]. Helquist et al. illustrated similar reactivity using Mn(OAc)₃ and DDQ for oxidation of allylic alcohols and benzylic alcohols to the corresponding aldehydes and ketones at mild reaction conditions [28]. Despite this selective oxidation methodology favors the regeneration of the organic oxidant, it still requires the presence of metal salts in the final liquid product. Earlier, we have proposed application of anthraquinones as a catalyst for non-metallic oxidation of alcohols, however, the reaction proceed at relatively high temperature with oxidation of activated alcohols [29].

Hereby, we propose the preparation and application of hybrid heterogeneous catalyst characterized by the presence of an organic shell in charge of the abstraction of hydrogen during the selective oxidation of alcohols to carbonyl compounds and a metallic core able to regenerate organic shell of the catalyst (**Scheme 1**). We have found that deposition of sulfonated anthraquinone over Ru nanoparticles in core-shell catalyst results in selective oxidation of alcohols to aldehydes. The alcohols are selectively oxidized (oxidatively dehydrogenated) over the non-metallic anthraquinone, whereas the production of water takes place on the metallic core, in presence of oxygen. This

system mimics the behavior of an electrochemical cell with oxidizing nano-anode in the form of the shell and reducing nano-cathode in the form of the core.

Experimental Section

Reagents

The chemicals $\text{RuCl}_3 \cdot \text{H}_2\text{O}$ (99.9 wt%, CAS: 14898-67-0), $\gamma\text{-Al}_2\text{O}_3$ (99 wt%, CAS: 1344-28-1), CTAB (99 wt%, CAS: 57-09-0), NaBH_4 (96 wt%, CAS: 16940-66-2), biphenyl (99.5 wt%, CAS: 92-52-4), benzyl alcohol (99 wt%, CAS: 100-51-6), 4-chlorobenzyl alcohol (98 wt%, CAS: 873-76-7), 4-methylbenzyl alcohol (98 wt%, CAS: 589-18-4), cinnamyl alcohol (98 wt%, CAS: 104-54-1), 1,2-hexanediol (98 wt%, CAS: 6920-22-5), furfuryl alcohol (98 wt%, CAS: 98-00-0), HMF (95 wt%, CAS: 67-47-0), 1-octanol (>99 wt%, CAS: 111-87-5), 2-octanol (98 wt%, CAS: 6920-22-5), cyclohexanol (99 wt%, CAS: 108-93-0), 1,4-benzoquinone (98 wt%, CAS: 106-51-4), 2-ethylanthraquinone (97 wt%, CAS: 84-51-5), 1,4-naphthoquinone (97 wt%, CAS: 130-15-4), anthraquinone-2-carboxylic acid (98 wt%, CAS: 117-78-2), disodium anthraquinone -2,6-disulfonate (95 wt%, CAS: 212-719-9) are purchased from J&K Scientific Ltd.

Synthesis of Catalysts

Reverse micellar microemulsions of CTAB/1-hexanol/water (as shown in **Table S1, SI**) have been prepared [15,]. Briefly, 10 g of microemulsion B containing 0.14 g NaBH_4 has been dropwise added to 10 g of microemulsion A containing 0.2 g RuCl_3 during 1 h under vigorous stirring. Ru nanoparticles with uniform size distribution have been formed inside the micelles. The catalyst **Ru NPs** has been separated by centrifugation, washed with hot water for 5 times and dried at 60 °C in vacuum oven for 12 h.

The catalysts **Ru@SQ** with varied shell thickness have been prepared by deposition of SQ over Ru NPs. Briefly, different amounts of SQ have been ultrasonically dissolved in 3 mL of water and subsequently mixed with 100 mg of Ru NPs. The water has been removed from resulting slurry by rotary evaporator and consequently dried at 60 °C in a vacuum oven overnight. A series of samples **Ru@SQ-X%** (X = 10, 25, 50 and 80) have been prepared, where X is the theoretical weight percentage of SQ. The sample with monolayer coating **Ru@SQ-monolayer** has been prepared by deposition of 2 wt. % of SQ over Ru NPs.

Catalyst Characterization

The morphologies and particle size distribution of the catalysts and elemental mapping analysis has been performed using JEOL 2100 high-resolution transmission electron microscope (HRTEM) with an accelerating voltage of 200 kV.

X-ray diffraction (XRD) was used to characterize the lattice structure. XRD patterns were recorded on a Rigaku D/max-2200/PC diffractometer using Cu K α radiation ($\lambda = 1.5418 \text{ \AA}$) operating at 20 kV.

X-ray photoelectron spectroscopy (XPS) spectra were acquired using a Thermo Scientific ESCALAB 250Xi X-ray Photoelectron Spectrometer incorporating a 165 mm hemispherical electron energy analyzer. The incident radiation is Monochromatic Al K α X-rays (1486.6 eV) at 225 W (15 kV, 15 ma). The deconvolution was performed on Thermo Scientific Avantage Software.

Thermogravimetric analysis (TGA) measurements were performed using a SDT 2960 analyzer from TA instrument under air flow (50 mL/min) with a ramping rate of temperature of 10 °C/min.

In-situ FTIR spectra were recorded using a Thermo Fisher Scientific Nicolet 6700 FTIR (16 scans at a resolution of 4 cm⁻¹) equipped with MCT detector, high-vacuum system and heating zone. The catalyst pellet has been pretreated at 150 °C for 1 h in vacuum at 10⁻⁵ Torr and cooled down to room temperature. The catalyst has been treated by 20 Torr hydrogen or furfuryl alcohol vapors at 25 °C~100 °C for 20 min.

The ¹H NMR spectra were measured using a Bruker ARX 400 or ARX 100 spectrometer at 400 MHz (¹H) and 100 MHz (¹³C).

Catalysis

The catalytic tests were conducted in a 30 mL autoclave. For a typical test of 1-octanol oxidation, 50 mg catalysts and 3 g of 1-octanol have been added in the reactor, which was pressurized with 10 bar of O₂ and heated to 100 °C for 1~48 h under continuous stirring. The reference experiments with Ru NPs, pure SQ and the mixture of Ru and SQ were carried out under the same reaction conditions. Other alcohols have been oxidized in a similar way.

The catalytic oxidation of aldehyde has been performed in the same autoclave. The catalysts containing 5 mg of Ru and 0.3 g of octanal were placed in the reactor with air

as oxidant at atmospheric pressure and solvent-free conditions. The mixture was stirred at 60 °C for 20 min.

The products of the reaction were analyzed using Agilent 7820A gas chromatography (GC) equipped with a HP-5 column and biphenyl as internal standard.

Cyclic voltammetry

Cyclic voltammetry (CV) was performed with a three-electrode setup controlled by a potentiostat (Reference 3000, Gamry Instruments Inc.). The synthesized catalysts containing Ru NPs or SQ were dispersed in ethanol to form a well-dispersed ink (10 mg/ml) using Nafion 117 solution (5 wt%) as a binder. 100 μ L of the ink was deposited onto a polished and pre-cleaned glassy-carbon electrode with a working area of 0.1256 cm². For Ru@SQ-80%, the working electrode was prepared by coating of electrode surface by 20 μ L Ru NPs and subsequently 80 μ L SQ ink. Ag/Ag⁺ was used as a reference electrode in all measurements while Pt wire as a counter electrode. CVs were carried out at 25 °C in 8 mL solution of 0.1 M LiClO₄ in DMSO saturated with Ar at a constant sweep rate of 100 mV/s.

Results and Discussion

Catalytic performances

Water-in-oil microemulsions built of water, hexanol and surfactant cetyltrimethylammonium bromide (CTAB) with RuCl₃ and sodium borohydride have been used for the synthesis of metal nanoparticles. Ru nanoparticles form aggregates and the size of Ru nanoparticles measured by TEM varies in the range 2-3 nm (**Figure 1**).

Ru@quinone catalysts with core-shell structure have been prepared using rotary evaporator for deposition of quinone over Ru nanoparticles by removal of solvent. The prepared samples are denoted as Ru@quinone-X % (X=10, 25, 50, 80), where X is the weight percentage of quinone in the samples. **Figure 1** demonstrates TEM images of Ru nanoparticles coated by different amount of disodium anthraquinone-2,6-disulfonate (SQ) in Ru@SQ catalysts. There is a clear contrast between the heavier atom of Ru in the core and the lighter SQ shell. Increase of the content of SQ phase leads to increase of the thickness of the shell from 1 to 3 nm.

The catalytic performance of core-shell catalysts with different content of SQ has been compared with the reference Ru nanoparticles and pure SQ in selective oxidation

of 1-octanol. Besides aldehyde as the main product of the reaction, there is an octanoic acid as the product of deeper oxidation of aldehyde and octyl octanoate as the product of further esterification (**Scheme 2**). 1-Octanol in the presence of acid also undergoes etherification reaction to dioctyl ether.

The catalytic activity of 1-octanol oxidation is the highest over Ru NPs with decrease of the activity after deposition of SQ (**Figure 2**). Increase of SQ loading leads to decrease of the catalytic activity. Almost no activity has been observed for pure SQ. Thus, presence of Ru NPs in the core of the catalyst affects the catalytic activity in alcohol oxidation. Comparison of the catalytic activity of core-shell Ru@SQ-80% with mechanical mixture Ru+SQ-80% indicates on SQ coating as the reason of low activity (**Figure 2**). It is interesting to note that activity normalized by Ru is comparable in a series of core-shell Ru@SQ catalysts (**Figure 2**). It means that the thickness of SQ coating does not affect the catalytic activity and the rate limiting step could be in Ru-SQ interface zone. Non-coated Ru NPs provide significantly higher activity indicating on different mechanism of oxidation with and without SQ coating.

The parent Ru NPs demonstrate (**Figure S1, SI**) strong decrease of the selectivity to octanal with increase of the conversion of 1-octanol with formation of acid and ester as side products. **Figure 3** shows comparison of the selectivities over Ru NPs with core-shell Ru@SQ catalysts at the similar conversions about 60 %. At this conversion, the selectivity to octanal is only about 20 % over Ru NPs. Pure SQ provided even lower selectivity due to intensive over-oxidation to acid and ester. It is interesting to note that the selectivity to octanal was gradually increasing with increase of the content of SQ in the core-shell catalysts from 30 % for Ru@SQ-10% to 74 % for Ru@SQ-80%. Thus, the selectivity increases up to 3 times in comparison with pure Ru NPs and SQ. The catalysts with low loading of SQ still could contain accessible Ru surface, which explains lower selectivity. High selectivity at high SQ loading could be explained by full coverage of Ru surface by SQ.

Usually the aldehyde formation during 1-octanol oxidation is accompanied by subsequent non-catalytic and catalytic oxidation, which results in the formation of acid and esters. In our previous study of alcohols oxidation over Ru NPs we have demonstrated protective role of RuO_x species from adsorption and deeper oxidation of aldehydes to acids [15]. Similarly, the presence of SQ coating markedly reduces the exposure of active Ru NPs, which is likely to suppress the deep catalytic oxidation reaction. In order to verify this concept, we have conducted oxidation of 1-octanol

using mechanical mixture of Ru NPs with 80 % of SQ (Ru+SQ-80%). It is interesting to note that the selectivity to aldehyde was significantly lower than in the case of core-shell system and comparable with Ru NPs.

SQ is almost insoluble in 1-octanol, however, it could be soluble during the catalytic reaction in the presence of water. The catalytic stability has been studied by separation of the catalyst Ru@SQ-80% after the first cycle with subsequent test using fresh 1-octanol for different reaction time to provide comparable conversions. **Figure S2, SI** demonstrates decrease of the selectivity to octanal from 75 to 37 % for the second cycle at the selectivity 23 % for pure Ru NPs. It means partial dissolution of SQ during the catalytic reaction, which makes catalytic performance similar to Ru NPs. It is interesting to note that the catalytic performance of Ru@SQ-80% after two cycles could be recovered by recoating of SQ shell (**Figure S2, SI**). It confirms solubility issue during the catalytic reaction for this composite material, however, provides simple way to recover the catalytic performance.

Characterization of Catalysts

Powder X-ray diffraction (XRD) has been used to study the crystallinity of the catalysts. **Figure S3, SI** demonstrates broad peaks at 38.4 °, 42.2 °, 43.8 °, 58.2 ° and 69.4 °, which correspond to (100), (002), (101), (102) and (110) planes, respectively, of the hexagonal close-packed (hcp) small size Ru metal nanoparticles. SQ does not change the patterns of Ru, however, increase of SQ content leads to appearance of new signals at 16.2°, 19.5° and 26.2° corresponding to the indices of (210), (201) and (301), respectively, of orthorhombic phase of crystalline SQ [30, 31].

The composition and thermal stability of the Ru NPs and Ru@SQ catalysts has been examined by TGA (**Figure S4, SI**). The curves show weight losses in two steps. At low temperature (25~300 °C) the weight loss is the result of removal of water, 1-hexanol and CTAB used for the catalyst preparation. Subsequently, the weight losses of about 45 wt%, 23 wt%, 14 wt% and 9 wt% for Ru@SQ-X% samples (X=80, 50, 25, 10), respectively, have been observed between 400 °C and 600 °C, which could be ascribed to the combustion of SQ layer. The lower weight loss in comparison with the theoretical content of SQ should be ascribed to the generation of sodium sulfate as a product of oxidation.

XPS analysis of Ru nanoparticles covered by SQ (monolayer and 80%) in comparison with Ru nanoparticles and pure SQ has been performed to investigate the

electronic state of the ruthenium species (**Figure 4**). According to the XPS analysis (**Table S2, SI**), the ratios of S/Ru in both Ru@SQ-monolayer and Ru@SQ-80% samples are 0.1:1.0 and 2.3:1.0, respectively, which correlates well with the difference in SQ loading. Ru 3p core level spectra show the presence of ruthenium in two oxidation states: metallic Ru⁰ (Ru 3p_{3/2} BE 462.0-463.3 eV) and lower contribution of oxidized Ru species with lower electronic density (Ru 3p_{3/2} BE 464.6-465.5 eV). This assignment was made according to earlier studies of various Ru compounds including metallic Ru, RuO₂ and Ru(OH)₃ demonstrating different Ru 3p_{3/2} BEs [32].

After SQ deposition over the surface of Ru NPs, the metallic Ru 3p doublet shifts to lower binding energy values. Additionally, the oxidized Ru peak appears demonstrating partial oxidation of Ru. Increase of SQ deposition leads to decrease of the intensity of Ru peaks due to the attenuation of Ru signal by SQ shell. It should be noted that with the increase of SQ coating the metal Ru 3p doublet shifts to lower binding energy values from 462.7 eV to 462 eV. This shift can be associated with the effect of electron transfer from SQ to Ru leading to increase of the electronic density over Ru.

Pure SQ sample demonstrates only one O 1s peak at 531.8 eV although it is expected to have two types of oxygen in SO₃²⁻ and C=O. Most probably it is due to the strong interaction and electron transfer between oxygen in SO₃²⁻ [30] and oxygen in C=O [31] groups in SQ. Ru NPs demonstrate a similar O 1s peak with 531.8 eV BE, which is associated with RuO₂ or surface Ru(OH)₃ [33]. SQ coating over Ru NPs leads to appearance of two additional peaks: the broad peak at 534.1 eV, which can be assigned to oxygen in sulfo groups [34], and well defined peak at 530.2 eV (529.8 eV after 80% SQ loading). The 530.2 eV peak we associate with the bridge Ru-O-SQ species, which appearance indicates strong interaction between SQ and Ru (**Scheme 3**). This peak is attenuated as well as Ru 3p doublet with the increase of SQ loading.

Structure-catalytic performances relationship

In order to understand the role of Ru in the core-shell catalyst for oxidation of alcohols, we have varied the metal core. We have used Pd and Pt nanoparticles prepared in the same way for subsequent deposition of SQ to check the effect of metal of the core on the catalytic performance during oxidation of 1-octanol. **Figure S5, SI** demonstrates selectivity-conversion curves for Pd@SQ and Pt@SQ catalysts with different content

of SQ in comparison with Pd and Pt nanoparticles. In comparison with Ru catalysts, the deposition of SQ over Pt and Pd leads either to low effect in selectivity or significant decrease of the selectivity to aldehyde with increase of the contribution of acid and ester.

Pt and Pd are well-known catalysts for hydrogenation/dehydrogenation reactions in comparison with Ru, which is used for hydrogenolysis reactions. Pt and Pd nanoparticles do not demonstrate strong interaction with SQ as demonstrated by XPS analysis of the samples before and after SQ impregnation (**Figure S6, SI**). The reason could be in strong oxophilicity of Ru leading to easy adsorption of oxygen on the surface with formation of Ru-O species. In order to confirm it, we have examined O 1s XPS spectra. SQ covered Pt and Pd nanoparticles in O 1s spectra do not show peak around 530 eV, which has been assigned to Me-O species (**Figure S7, SI**). Pd 3d and Pt 4f spectra demonstrate the metallic state of the elements with no changes after SQ loading. Thus, one can conclude that there is no interaction between Pt or Pd and SQ in contrast to Ru nanoparticles.

Thus, strong interaction of Ru with SQ could be the key factor of high selectivity during oxidation of alcohols to carbonyl compounds. The mechanism of the reaction has been further studied using FTIR and electrochemical methods.

Mechanism

According to our earlier studies, oxidation of alcohols over Ru nanoparticles proceed according to Mars-van Krevelen mechanism by interaction of surface RuO_x species over Ru nanoparticles with alcohol leading to the aldehyde formation and subsequent re-oxidation of Ru nanoparticles [15]. In order to verify if SQ could be involved in this mechanism of oxidation of alcohols, we have performed the 1-octanol oxidation reaction in inert atmosphere. The only product of the reaction is octanal. **Figure 5** demonstrates the conversion of 1-octanol depending on the content of SQ in the catalyst. The yield of octanal was gradually decreasing from 9 to 1 % with increase of the content of SQ up to 80 %. It indicates on different mechanism of alcohol oxidation in this case and absence of direct contact of 1-octanol with Ru core.

In addition, considering alcohols oxidation to acids as consecutive reaction with intermediate aldehydes formation, the higher selectivity to octanal could be explained by suppression of further aldehyde oxidation over core-shell catalysts. In order to support this assumption, we have performed model reaction of octanal oxidation at mild reaction conditions to avoid autoxidation (**Figure 6**). Blank experiments without Ru

species show almost no conversion of octanal at 60 °C and air instead of oxygen. Ru NPs provide conversion of octanal 26 % to acid. Increase of the amount of coated SQ leads to suppression of octanal oxidation and correlates with the results of 1-octanol accessibility to Ru core. It proves that SQ shell protects Ru core from interaction with aldehydes and suppresses over-oxidation, which could be the reason of high selectivity.

The key question in this case is how Ru@SQ catalyst provides oxidative dehydrogenation of alcohols. In-situ FTIR has been used to study the state of SQ during interaction with alcohol. FTIR spectrum of parent SQ (**Figure 7**) shows the peak at 1277 cm^{-1} attributed to the sulfonate group [30]. The peak at 1514 cm^{-1} can be assigned to the stretching vibration of aromatic conjugate C=C band [35]. The strong characteristic peaks at 1695 cm^{-1} and 1624 cm^{-1} can be assigned to the stretching C=O vibrations in non-chelated and a chelated quinone carbonyl group, respectively [36]. The non-chelated quinone group disappears after core-shell structure fabrication, which could be explained by strong interaction between C=O and Ru NPs in accordance with XPS results (**Figure 4**). It is interesting to note that the spectrum of mechanical mixture of SQ with Ru is similar to pure SQ and confirms specific interaction of SQ with Ru only in core-shell material (**Figure S8, SI**).

Presence of hydrogen in IR cell leads to decrease of the intensity of the C=O group at 1624 cm^{-1} , which could be recovered after the heating treatment at 100 °C in vacuum. It indicates on easy reduction of C=O to C-OH and subsequent decomposition in the absence of hydrogen.

Pure SQ and mechanical mixture of SQ with Ru does not show any interaction with hydrogen (**Figure S8, SI**). Hydrogenation of SQ could be initiated by hydrogen dissociation over Ru [37] with subsequent hydrogen transfer to SQ through Ru-O-SQ linkers. In order to study hydrogen transfer from alcohol molecule, we have introduced furfuryl alcohol vapors in the cell with subsequent heating from 25 to 100 °C (**Figure 7**). The carbonyl group characterized by the peak located at 1624 cm^{-1} started to decrease in intensity at 80 °C in comparison with no effect for pure SQ or mechanical mixture Ru+SQ-80% (**Figure S8, SI**). Thus, carbonyl group of SQ in core-shell catalyst can be involved in hydrogen transfer from alcohol with generation of aldehyde and hydrogenated carbonyl group in the shell. Subsequent transfer of hydrogen through carbonyl group of SQ to Ru and decomposition with regeneration of C=O in SQ could be proposed as mechanism of oxidation of alcohols without direct contact of metal with alcohol (**Scheme 1**).

The advantage of SQ in comparison with the strong electrophilic organic scavengers like TEMPO or DDQ is its intermediate reduction potential leading to lower stability of hydrogenated form, which results in efficient hydrogen transfer and regeneration of SQ over Ru surface.

Electrochemical experiments have been used to further evaluate the state of SQ in the core-shell catalyst. Cyclic voltammograms (CVs) of the bare glassy carbon (GC) electrode, Ru NPs/GC, SQ/GC, and Ru@SQ-80%/GC electrodes in Ar-saturated DMSO solution with 0.1 M LiClO₄ as electrolyte were studied in the presence/absence of 0.1 M furfuryl alcohol (FA). The cyclic voltammetry data for SQ are characterized by two anodic and cathodic waves between -1.6 V and -1 V vs Ag/Ag⁺ corresponding to the two consecutive one-electron reversible transfer process of the oxydo-reduction of anthraquinones to hydroquinone (**Figure 8, Table 1**). However, when 0.1 M of furfuryl alcohol (FA) is added a 3rd anodic wave occurs at -0.14 V for SQ-FA and at -0.21 V for Ru@SQ-80%-FA corresponding to the oxidation of FA.

At the same time, blank Ru NPs/GC and bare GC electrodes have no CVs responses (**Figure S9, SI**). For the Ru@SQ-80%-FA, the lowest oxydo-reduction peak around -1.62 V shifts to higher voltage -1.25 V, which shows that only one electron transfer is involved in the oxidation of FA. This leads to increase of the current density of FA oxidation at -0.21 V. Moreover, the resulting current density for FA oxidation over Ru@SQ-80% is much higher in comparison with pure SQ. The negative shift and higher current density of this peak for Ru@SQ-80% combined with the shift of the peak of SQ to higher voltages indicates increase of the catalytic activity of Ru@SQ-80% in comparison to pure SQ for the oxidation of FA. The improved electrocatalytic activity in oxidation of FA could be due to the presence of Ru in the core, which accelerates the electron transfer via improved conductivity and change of the electronic state of SQ in the core-shell catalyst observed by FTIR and XPS.

Substrate Scope

The selective oxidation of a wide range of alcohols has been studied over Ru@SQ-80% catalyst in the presence of O₂. For benzyl alcohol, methyl-substituted and chlorinated benzylic alcohol conversions of 92 %, 95 % and 95 % have been achieved within 6 h, respectively (**Table 2**). The selectivity to the target products was higher than 95 %. Similarly, unsaturated cinnamyl alcohol was converted to cinnamaldehyde with 95 % selectivity. In the case of oxidation of furfuryl alcohol and 2,5-

hydroxymethylfurfural (HMF) the selectivity about 90 % was achieved to furfural and 2,5-diformylfuran (DFF), respectively, at high conversion. Non-activated aliphatic alcohol (i.e., 1-octanol) and cyclic alcohol (i.e., cyclohexanol) over Ru@SQ-80% have been converted to carbonyl compounds with a moderate activity and excellent selectivity. Secondary 2-octanol, can be oxidized with a conversion of >90 % and selectivity of 95 % to corresponding ketone, which is comparable to the selectivity achieved using TEMPO [38].

The excellent catalytic activity towards various oxygenate substrates demonstrates that the uniform organic shell around the metal nanoparticles suppressed over-oxidation of aldehydes toward acids and esters. Nanocell Ru@SQ exhibits much better catalytic behavior than conventional Ru catalysts [39]. Isolation of metal nanoparticles from direct contact with alcohols decreases activity, however, results in significant increase of the selectivity toward carbonyl compounds. The catalytic system can be further optimized by variation of the shell type for more efficient alcohols dehydrogenation and hydrogen transfer to combine high activity and selectivity of the catalyst.

Conclusion

In conclusion, we have demonstrated that it is possible to build nanocell with core-shell structure containing Ru nanoparticles in the core and electro-deficient anthraquinones in the shell for selective oxidation of alcohols to carbonyl compounds. XPS analysis shows strong interaction between quinone species and Ru nanoparticles leading to transfer of the electronic density to Ru and easy activation of alcohols over the shell. In-situ mechanism study confirms transfer of hydrogen to carbonyl groups of quinone species from alcohol with subsequent transfer to the core. This concept can be used for other applications, where contact of the target product of the reaction with metal results in decrease of the selectivity.

Declaration of interests

The authors declare that they have no known competing financial interests or personal relationships that could have appeared to influence the work reported in this paper.

Acknowledgments

J.P. Zhao thanks Solvay and CIFRE (2016-1082) for providing him a stipend for PhD study

CRedit authorship contribution statement

V. Ordonsky, W.Y. Hernández and M. Capron conceived the idea for this work. All authors contributed to the design of the experimental set-up and experimental procedures. J.P. Zhao and W.J. Zhou prepared the catalysts and performed catalytic tests. Y. Yang and E.I. Vovk performed XPS analysis. M. Wu and N. Naghavi performed electrochemical measurements. J.P. Zhao and V. Ordonsky wrote the draught, and all the authors worked on improving the manuscript

References

- [1] Steven L. R., C. Koteel, Activation through impregnation. Permanganate-coated solid supports, *J. Am. Chem. Soc.*, 99 (1977) 3837-3838.
- [2] J. Muzart, Chromium-Catalyzed Oxidations in Organic Synthesis, *Chem. Rev.*, 92 (1992) 113-140.
- [3] F. M. Perree, A. Gaudemer, Manganese Porphyrin-catalysed Oxidation of Olefins to Ketones by Molecular Oxygen, *J. Chem. Soc. Chem. Commun.*, 1282 (1981) 874-875.
- [4] Uyanik M., I. K., Hypervalent Iodine-mediated Oxidation of Alcohols, *Chem. Commun.*, 1 (2009) 2086-2099.
- [5] I. Satoshi, K. Koji, I. Shigeru, M. Teruaki, A New and Facile Method for the Direct Preparation of α -Hydroxycarboxylic Acid Esters from α,β -Unsaturated Carboxylic Acid Esters with Molecular Oxygen and Phenylsilane, *Chem. Lett.*, 19 (1990) 1869-1872.
- [6] W. Zhai, S. Xue, A. Zhu, Y. Luo, Y. Tian, Plasmon-Driven Selective Oxidation of Aromatic Alcohols to Aldehydes in Water with Recyclable Pt/TiO₂ Nanocomposites, *ChemCatChem.*, 3 (2011) 127-130.
- [7] M. Ilyas, M. Sadiq, Liquid-Phase Aerobic Oxidation of Benzyl Alcohol Catalyzed by Pt/ZrO₂, *Chem. Eng. Technol.*, 30 (2007) 1391-1397.
- [8] J. Xie, B. Huang, K. Yin, H.N. Pham, R.R. Unocic, A.K. Datye, R.J. Davis, Influence of Dioxygen on the Promotional Effect of Bi during Pt-Catalyzed Oxidation of 1,6-Hexanediol, *ACS Catal.*, 6 (2016) 4206-4217.
- [9] S.F. Hackett, R.M. Brydson, M.H. Gass, I. Harvey, A.D. Newman, K. Wilson, A.F. Lee, High-activity, single-site mesoporous Pd/Al₂O₃ catalysts for selective aerobic oxidation of allylic alcohols, *Angew. Chem. Int. Ed.*, 46 (2007) 8593-8596.
- [10] C.M.A. Parlett, D.W. Bruce, N.S. Hondow, A.F. Lee, K. Wilson, Support-Enhanced Selective Aerobic Alcohol Oxidation over Pd/Mesoporous Silicas, *ACS Catal.*, 1 (2011) 636-640.
- [11] G. Zhao, M. Ling, H. Hu, M. Deng, Q. Xue, Y. Lu, An excellent Au/meso- γ -Al₂O₃ catalyst for the aerobic selective oxidation of alcohols, *Green Chem.*, 13 (2011) 3088-3092.

- [12] A. Tanaka, K. Hashimoto, H. Kominami, Preparation of Au/CeO₂ exhibiting strong surface plasmon resonance effective for selective or chemoselective oxidation of alcohols to aldehydes or ketones in aqueous suspensions under irradiation by green light, *J. Am. Chem. Soc.*, 134 (2012) 14526-14533.
- [13] J. Nie, J. Xie, H. Liu, Efficient aerobic oxidation of 5-hydroxymethylfurfural to 2,5-diformylfuran on supported Ru catalysts, *J. Catal.*, 301 (2013) 83-91.
- [14] G. Wang, U. Andreasson, J.E. Backval, Aerobic oxidation of secondary alcohols via ruthenium-catalysed hydrogen transfer involving a new triple catalytic system, *J. Am. Chem. Soc.*, 4 (1994) 1037-1039.
- [15] J. Zhao, W.Y. Hernández, W. Zhou, Y. Yang, E. Vovk, M. Capron, V. Ordonsky, Selective oxidation of alcohols to carbonyl compounds over small size colloidal Ru nanoparticles, *ChemCatChem*, (2019).
- [16] A.C. Schmidt, C.B.W. Stark, TPAP-Catalyzed Direct Oxidation of Primary Alcohols to Carboxylic Acids through Stabilized Aldehyde Hydrates, *Org. Lett.*, 13 (2011) 4164-4167.
- [17] W.Y. Hernandez, A. Hadjar, A. Giroir-Fendler, P. Andy, A. Princivalle, M. Klotz, A. Marouf, C. Guizard, C. Tardivat, C. Viazzi, Electrochemically-assisted NO_x storage–reduction catalysts, *Catal. Today*, 241 (2015) 143-150.
- [18] G.R.A. Adair, J.M.J. Williams, Oxidant-free oxidation: ruthenium catalysed dehydrogenation of alcohols, *Tetrahedron Lett.*, 46 (2005) 8233-8235.
- [19] A. Deffernez, S. Hermans, M. Devillers, Bimetallic Bi–Pt, Ru–Pt and Ru–Pd and trimetallic catalysts for the selective oxidation of glyoxal into glyoxalic acid in aqueous phase, *Appl. Catal. A: Gen.*, 282 (2005) 303-313.
- [20] K. Mori, T. Hara, T. Mizugaki, K. Ebitani, K. Kaneda, Hydroxyapatite-Supported Palladium Nanoclusters: A Highly Active Heterogeneous Catalyst for Selective Oxidation of Alcohols by Use of Molecular Oxygen, *J. Am. Chem. Soc.*, 126 (2004) 10657-10666.
- [21] S. Hosokawa, Y. Hayashi, S. Imamura, K. Wada, M. Inoue, Effect of the Preparation Conditions of Ru/CeO₂ Catalysts for the Liquid Phase Oxidation of Benzyl Alcohol, *Catal. Lett.*, 129 (2009) 394-399.
- [22] B.L. Ryland, S.S. Stahl, Practical Aerobic Oxidations of Alcohols and Amines with Homogeneous Copper/TEMPO and Related Catalyst Systems, *Angew. Chem. Int. Ed.*, 53 (2014) 8824-8838.
- [23] S. Ma, J. Liu, S. Li, B. Chen, J. Cheng, J. Kuang, Y. Liu, B. Wan, Y. Wang, J. Ye, Q. Yu, W. Yuan, S. Yu, Development of a General and Practical Iron Nitrate/TEMPO-Catalyzed Aerobic Oxidation of Alcohols to Aldehydes/Ketones: Catalysis with Table Salt, *Adv. Synth. Catal.*, 353 (2011) 1005-1017.
- [24] K. Walsh, H.F. Sneddon, C.J. Moody, Solar photochemical oxidations of benzylic and allylic alcohols using catalytic organo-oxidation with DDQ: Application to lignin models, *Org. Lett.*, 16 (2014) 5224-5227.
- [25] Y. Hu, L. Chen, B. Li, Fe (NO₃)₃/2, 3-dichloro-5, 6-dicyano-1, 4-benzoquinone (DDQ): An efficient catalyst system for selective oxidation of alcohols under aerobic conditions, *Catal. Commun.*, 103 (2018) 42-46.
- [26] R. Liu, X. Liang, C. Dong, X. Hu, Transition-metal-free: A highly efficient catalytic aerobic alcohol oxidation process, *J. Am. Chem. Soc.*, 126 (2004) 4112-4113.
- [27] J.W. Scott, D.R. Parrish, F.T. Bizzarro, A Rapid and Mild Process for the Oxidation of 2, 3-Dichloro-5, 6-dicyanobenzoquinone (DDQ) from 2, 3-Dichloro-5, 6-dicyanohydroquinone (DDHQ), *Org. Prep. Proced. Int.*, 9 (1977) 91-94.
- [28] C.C. Cosner, P.J. Cabrera, K.M. Byrd, A.M.A. Thomas, P. Helquist, Selective Oxidation of Benzylic and Allylic Alcohols Using Mn(OAc)₃/Catalytic 2, 3-Dichloro-5, 6-dicyano-1, 4-benzoquinone, *Org. Lett.*, 13 (2011) 2071-2073.

- [29] J. Zhao, D. Wu, W.Y. Hernández, W.-J. Zhou, M. Capron, V.V. Ordonsky, Non-metallic Aerobic Oxidation of Alcohols over Anthraquinone Based Compounds, *Applied Catalysis A: General*, 590 (2020) 117277.
- [30] J. Zhao, J. Yang, P. Sun, Y. Xu, Sodium sulfonate groups substituted anthraquinone as an organic cathode for potassium batteries, *Electrochem. Commun.*, 86 (2018) 34-37.
- [31] B. Peake, J. Simpson, X-Ray crystal structure determination of some sodium anthraquinone sulfonate derivatives, *Aust. J. Chem.*, 46 (1993) 1595-1604.
- [32] D.J. Morgan, Resolving ruthenium: XPS studies of common ruthenium materials, *Surf. Interface Anal.*, 47 (2015) 1072-1079.
- [33] A. Ananth, M.S. Gandhi, Y.S. Mok, A dielectric barrier discharge (DBD) plasma reactor: an efficient tool to prepare novel RuO₂ nanorods, *J. Phy. D.: Appl. Phys.*, 46 (2013) 155202-155210.
- [34] Y. Lim, Y. Tan, H. Lim, N. Huang, W. Tan, M.A. Yarmo, C.-Y. Yin, Potentiostatically deposited polypyrrole/graphene decorated nano-manganese oxide ternary film for supercapacitors, *Ceram. Int.*, 40 (2014) 3855-3864.
- [35] Y. Wang, T. He, M. Liu, J. Ji, Y. Dai, Y. Liu, L. Luo, X. Liu, J. Qin, Fast and efficient oil-water separation under harsh conditions of the flexible polyimide aerogel containing benzimidazole structure, *Colloid Surf. A*, 581 (2019) 123809-123810.
- [36] G.P. Demagos, W. Baltus, G. Höfle, New anthraquinones and anthraquinone glycosides from *Morinda lucida*, *Zeitschrift für Naturforschung B*, 36 (1981) 1180-1184.
- [37] F. Rose, M. Tatarkhanov, E. Fomin, M. Salmeron, Nature of the dissociation sites of hydrogen molecules on Ru (001), *J. Phys. Chem. C*, 111 (2007) 19052-19057.
- [38] Cecchetto A., Fontana F., Miniscia F., R. F., Efficient Mn–Cu and Mn–Co–TEMPO-catalysed oxidation of alcohols into aldehydes and ketones by oxygen under mild conditions, *Tetrahedron Lett.*, 42 (2001) 6651–6653.
- [39] V.C. Corberán, M.E. González-Pérez, S. Martínez-González, A. Gómez-Avilés, Green oxidation of fatty alcohols: Challenges and opportunities, *Appl. Catal. A: General*, 474 (2014) 211-223.

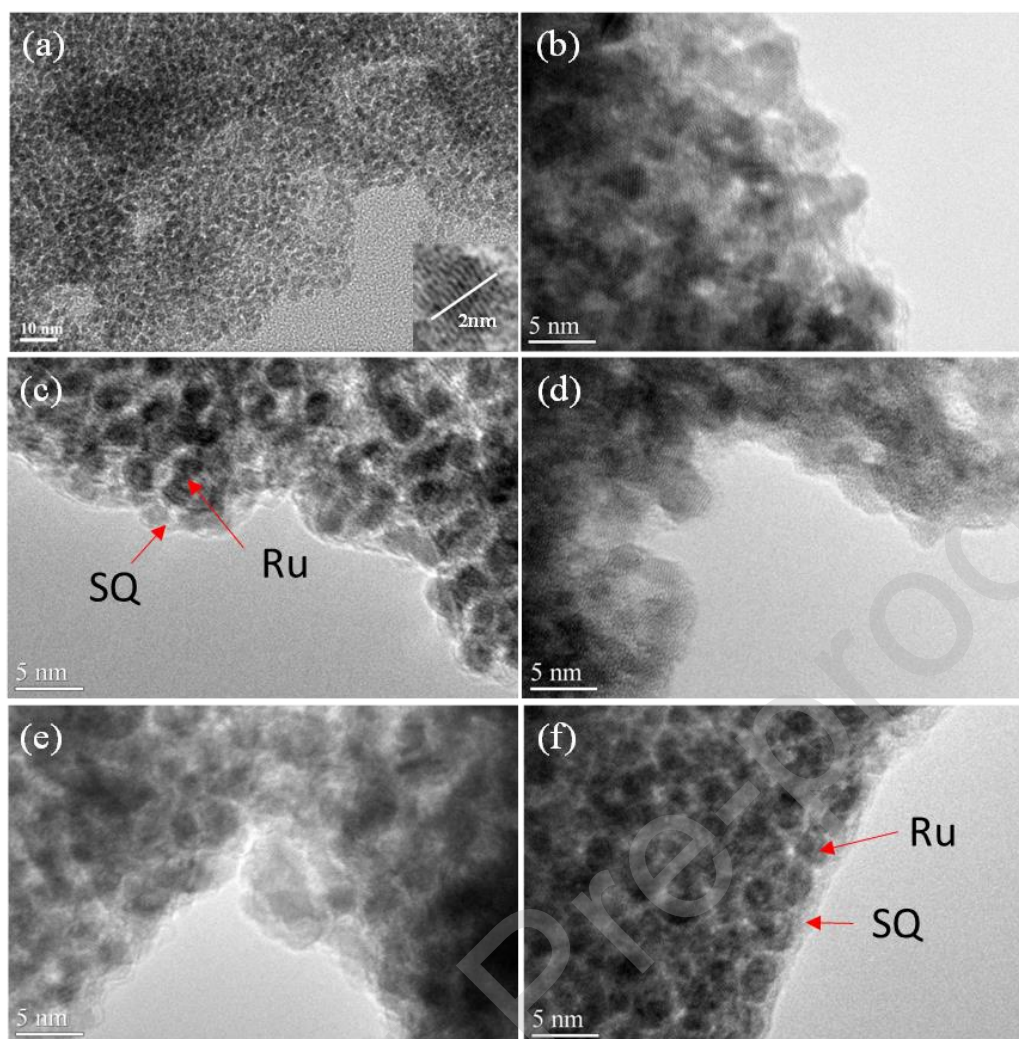


Figure 1. TEM images of (a) Ru NPs; (b) SQ; (c~f) Ru@SQ-X% catalysts, X=10, 25, 50, 80.

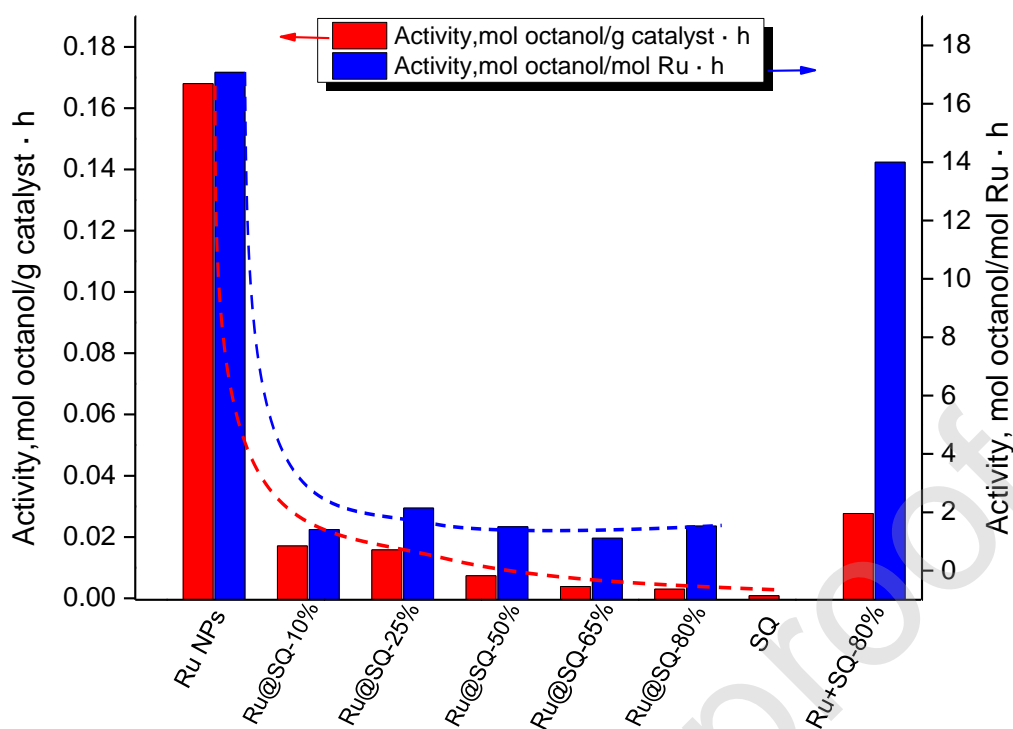


Figure 2. The catalytic activity of 1-octanol oxidation over different catalysts. The activity was calculated at low conversion (~15%) by the converted moles of 1-octanol (red) per gram of the whole catalyst per hour; (blue) per mol of Ru per hour. Reaction conditions: 3.0 g 1-octanol, 50 mg catalyst, solvent-free, $p(O_2)=10$ bar, $T=100$ °C, 1~36h.

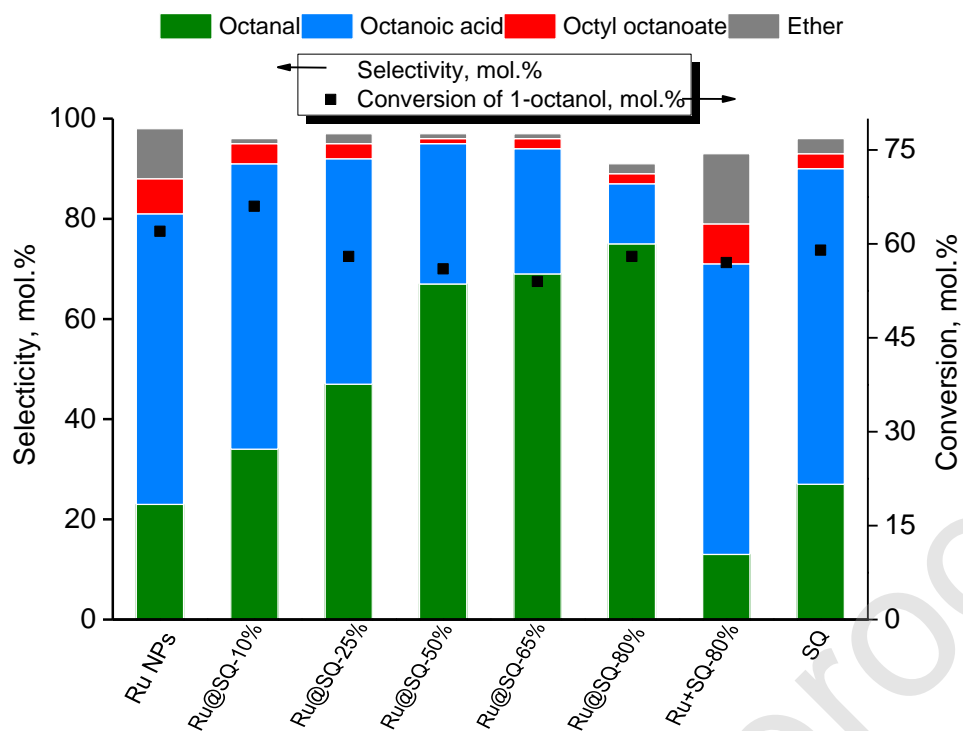


Figure 3. The selectivity during 1-octanol oxidation over different catalysts. Reaction conditions: 3.0 g 1-octanol, 50 mg catalyst, solvent-free, $p(O_2)=10$ bar, $T=100$ °C, 1~36 h.

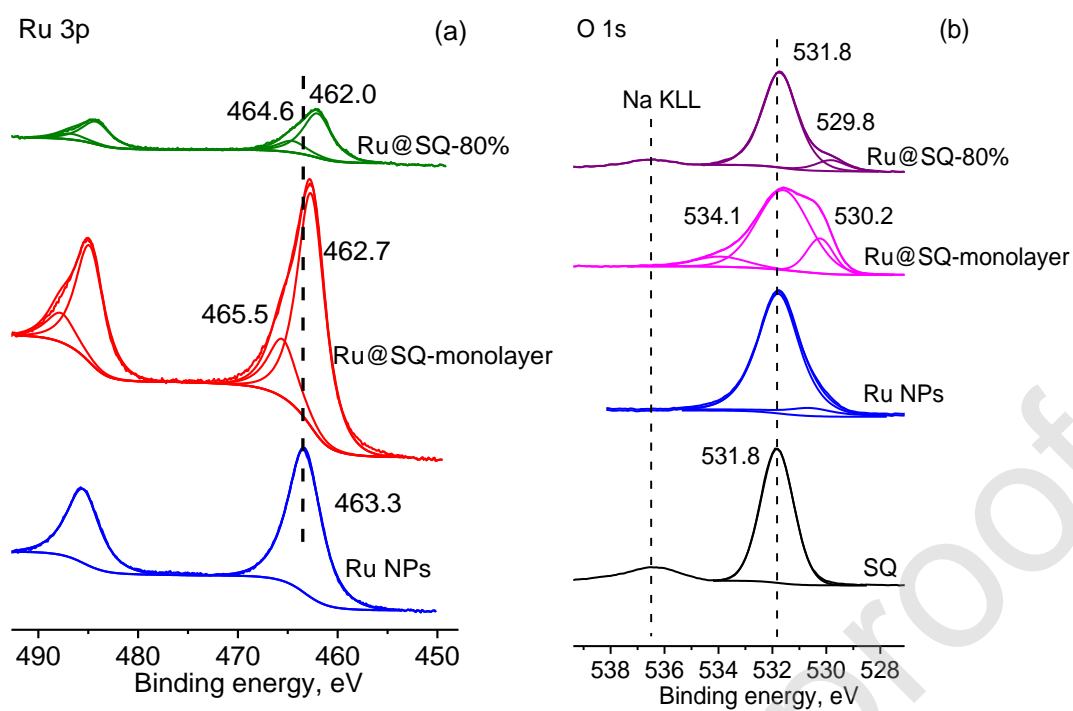


Figure 4. XPS spectra of Ru NPs, Ru@SQ-monolayer and Ru@SQ-80%. (a) Ru 3p, (b) O 1s core level spectra.

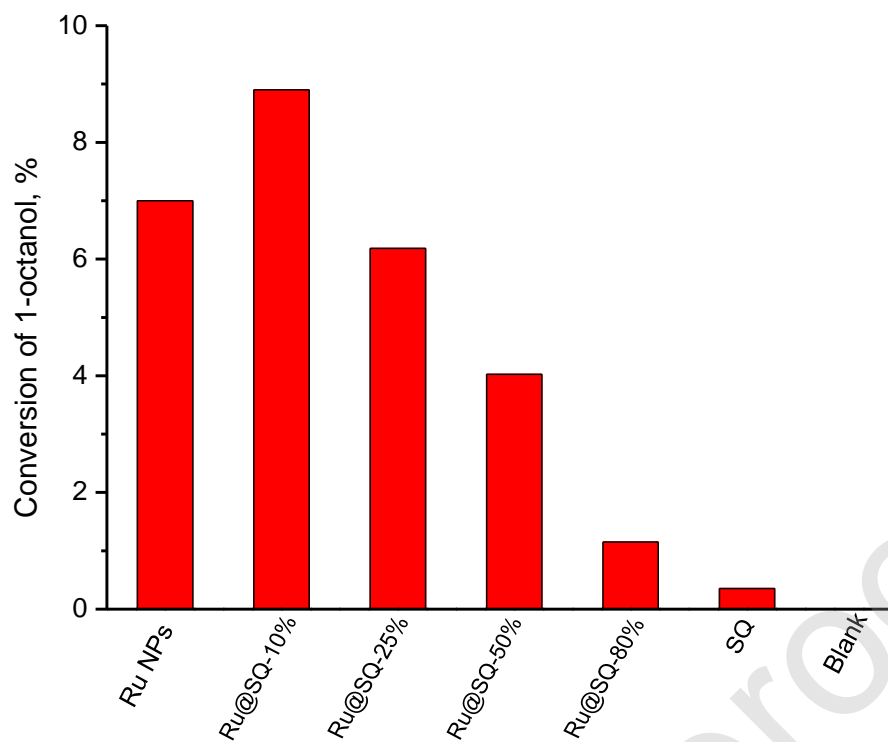


Figure 5. Oxidation of alcohol by Ru NPs, pure SQ and Ru@SQ-X% catalysts in inert atmosphere. Reaction conditions: amount of catalyst equivalent to 50 mg of Ru, 0.1 g 1-octanol, 2.0 g toluene as solvent, $T=100\text{ }^{\circ}\text{C}$, 3 h.

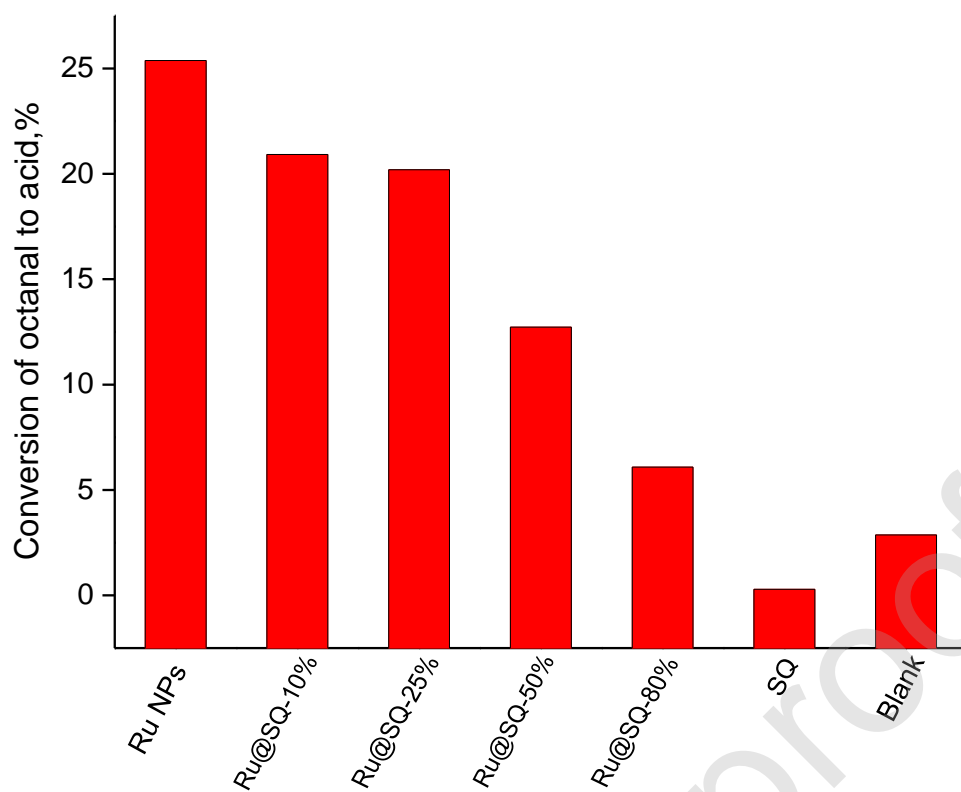


Figure 6. Oxidation of 1-octanal with different catalysts. Reaction conditions: amount of catalyst equivalent to 5 mg of Ru, 0.3 g octanal, solvent-free, air atmospheric pressure, $T=60\text{ }^{\circ}\text{C}$, 20 min.

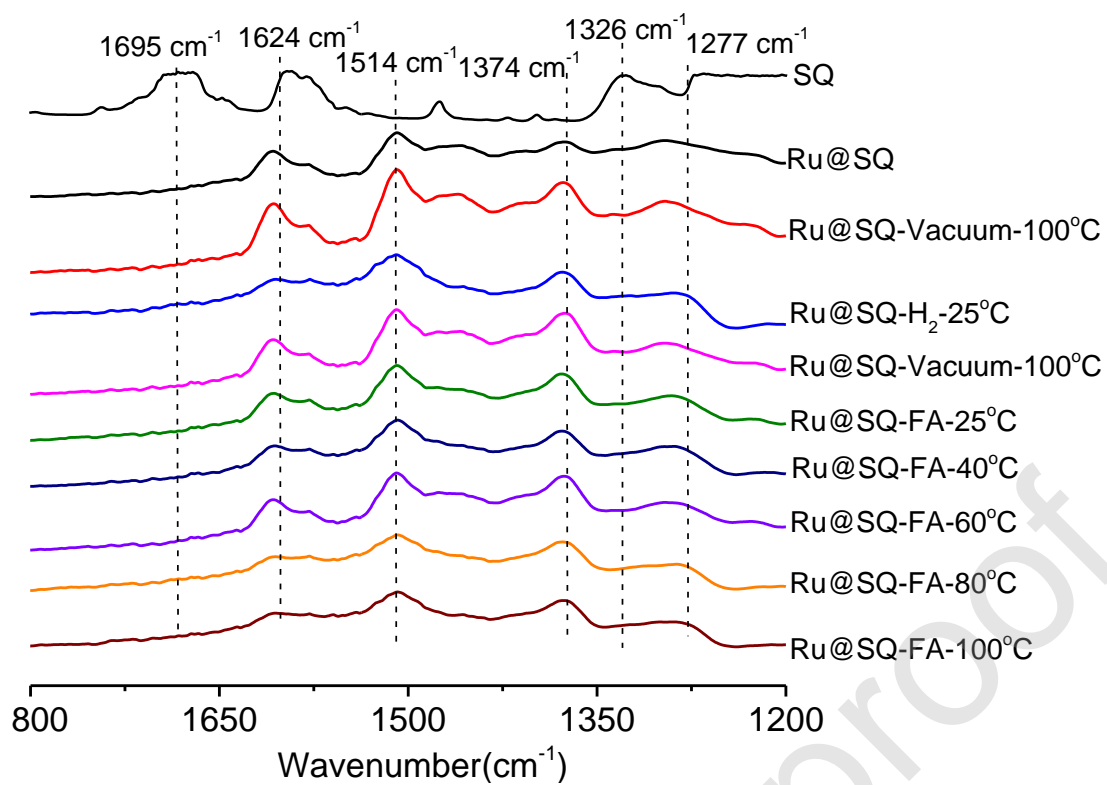


Figure 7. In-situ IR spectra of Ru@SQ-80% by H₂ and furfuryl alcohol (FA) treatment at different temperatures

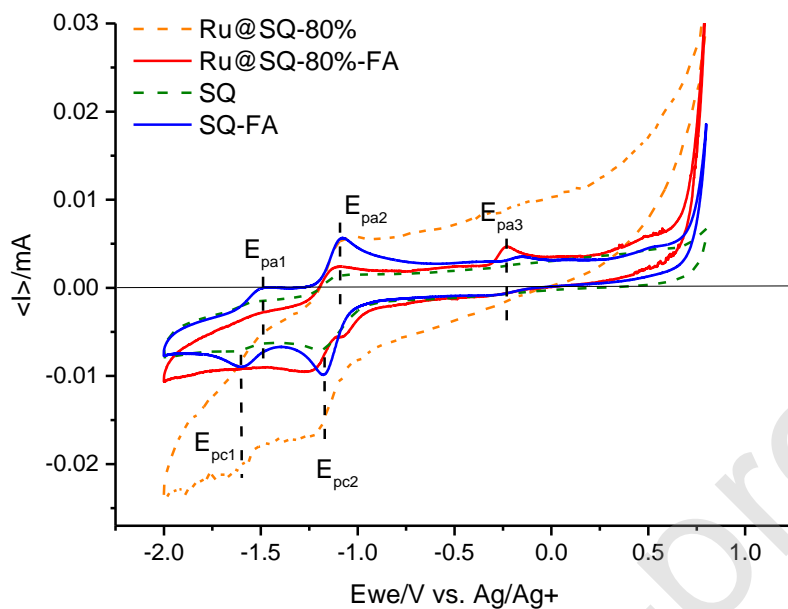
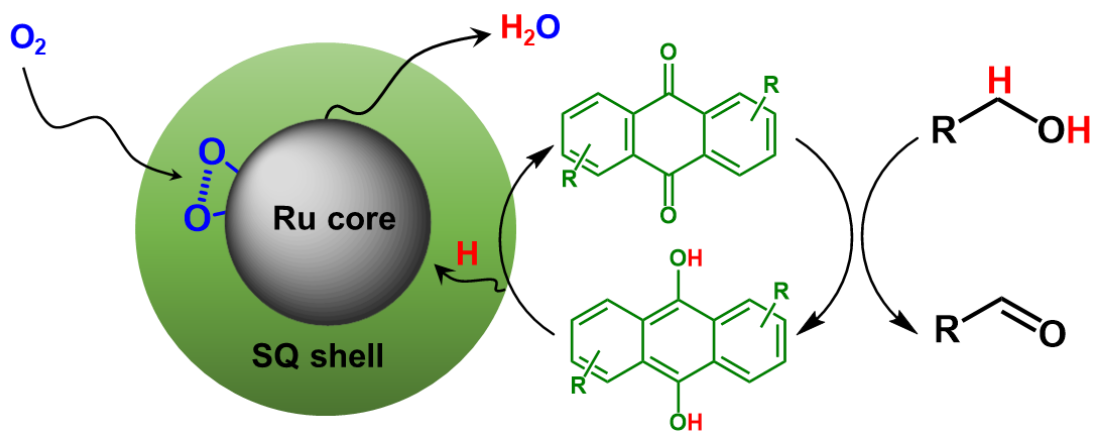
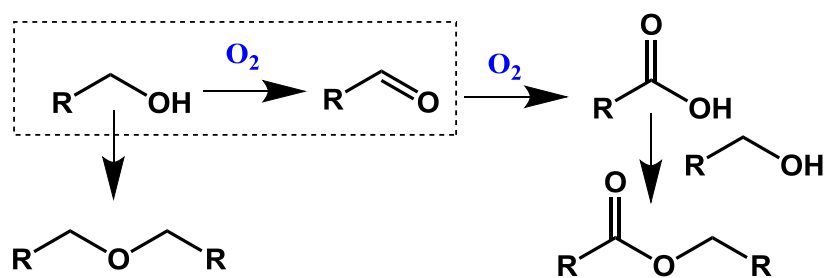


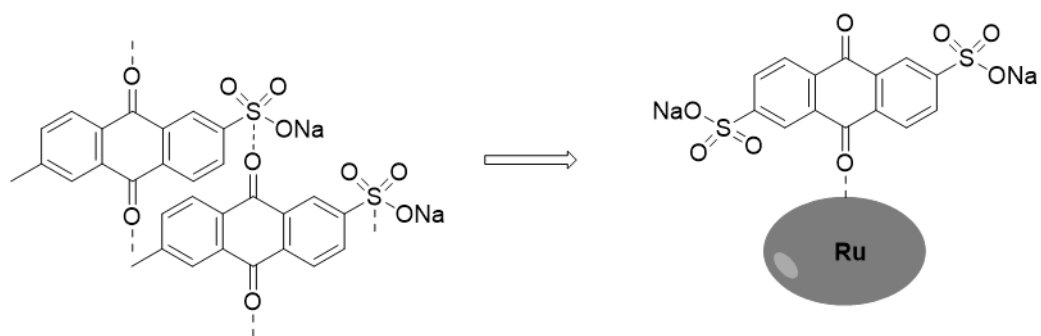
Figure 8. Cyclic voltammograms of the studied catalysts on a glassy carbon electrode in 0.1 M $LiClO_4$ in the DMSO solution with/without 0.1 M furfuryl alcohol (FA) inside in the range of -2.0 to 0.8 V at 100 mV/s scan rate.



Scheme 1. Proposed mechanism of alcohol oxidation by nanocells.



Scheme 2. *The reaction of alcohols oxidation.*



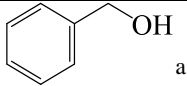
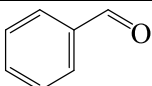
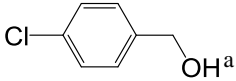
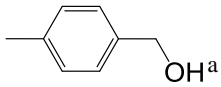
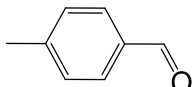
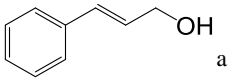
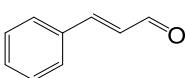
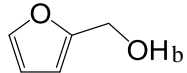
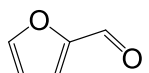
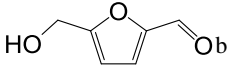
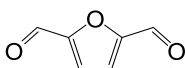
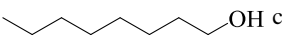
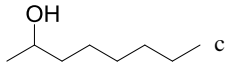
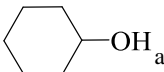
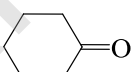
Scheme 3. Scheme of interaction between Ru and SQ.

Journal Pre-proof

Table 1. The values of cathodic E_{pc} and anodic E_{pa} peak potentials in DMSO solution.

	Anodic potential (V vs. Ag/Ag ⁺)			Cathodic potential (V vs Ag/Ag ⁺)	
	E _{pa1}	E _{pa2}	E _{pa3}	E _{pc1}	E _{pc2}
SQ	-1.54	-1.13		-1.62	-1.19
SQ-FA	-1.51	-1.08	-0.14	-1.61	-1.18
Ru@SQ-80%	-1.56	-1.11		-1.71	-1.22
Ru@SQ-80%-FA	-1.12		-0.21	-1.25	-1.05

Table 2. Substrate scope oxidation by Ru@SQ-80%

Alcohols	Alcohols /g	Target Molecule	T /°C	Time /h	Conv /%	Sele. /%
	1.0		100	6	92	95
	1.0		100	6	95	95
	1.0		100	6	95	95
	1.0		100	18	90	95
	0.5		90	3	80	92
	0.4		110	16	69	89
	3.0		100	36	57	74
	1.0		115	60	>90	>90
	1.0		115	60	>90	>90

^a Reaction conditions: catalyst 50.0 mg, toluene 2.0 g as solvent.

^b Reaction conditions: catalyst 50.0 mg, toluene 1.0 g + ethanol 1.0 g as solvent.

^c Reaction conditions: catalyst 50.0 mg, solvent-free.